
Article:
Janas, K., Łatkiewicz, A., Parnell, A. orcid.org/0000-0001-8606-8644 et al. (6 more authors) (2020) Differential effects of early growth conditions on colour-producing nanostructures revealed through small angle X-ray scattering (SAXS) and electron microscopy. The Journal of Experimental Biology, 223 (18). jeb.228387. ISSN 0022-0949

https://doi.org/10.1242/jeb.228387

Differential effects of early growth conditions on colour-producing nanostructures revealed through small angle X-ray scattering (SAXS) and electron microscopy

Katarzyna Janas[1*], Anna Łatkiewicz[2], Andrew Parnell[3], Dorota Lutyk[1], Julia Barczyk[1], Matthew D. Shawkey[4], Lars Gustafsson[5], Mariusz Cichoń[1], Szymon M. Drobniak[1,6]

1. *Institute of Environmental Sciences, Jagiellonian University, Kraków, Poland*
2. *Institute of Geological Sciences, Jagiellonian University, Kraków, Poland*
3. *Department of Physics and Astronomy, The University of Sheffield, United Kingdom*
4. *Evolution and Optics of Nanostructures, Department of Biology, University of Gent, Belgium*
5. *Department of Animal Ecology/Ecology and Genetics, Uppsala University, Uppsala, Sweden*
6. *School of Biological, Environmental and Earth Sciences, University of New South Wales, Sydney, Australia*

*Corresponding author

e-mail: k.janas@doctoral.uj.edu.pl

Abstract

The costs associated with the production and maintenance of colour patches is thought to maintain their honesty. Although considerable research on sexual selection has focused on structurally coloured plumage ornaments, the proximate mechanisms of their potential condition-dependence, and thus their honesty, is rarely addressed, particularly in an experimental context. Blue tit (*Cyanistes caeruleus*) nestlings have UV-blue structurally coloured tail feathers, providing a unique opportunity for investigation of the causes of variation in their colour. Here, we examined the influence of early growing conditions on reflectance and structural properties of UV-blue coloured tail feathers of blue tit nestlings. We applied a two-stage brood size manipulation to determine which stage of development more strongly impacts the quality of tail feather colouration and microstructure. We used small angle X-ray scattering (SAXS) and electron microscopy to characterize nano- and micro-scale structure of tail feather barbs. Nestlings from the broods enlarged at a later stage of growth showed a sex-specific rectrix development delay, with males being more sensitive to this manipulation. Contrary to predictions, treatment affected neither the quality of the barb's nanostructures nor the brightness and UV chroma of feathers. However, at the micro-scale, barb's keratin characteristics were impaired in late-enlarged broods. Our results suggest that nanostructure quality, which determines UV-blue colour in tail feathers, is not sensitive to early rearing conditions. Furthermore, availability of resources during feather growth seems to impact the quality of feather microstructure more than body condition, which is likely determined at an earlier stage of nestling growth.

Introduction

Birds are among the most vividly coloured animals, with conspicuous plumage produced by wavelength-specific absorption of pigments deposited in the feathers, by interaction of light with nanometer-scale structures inside feather barbs or barbules, or by combination of these two mechanisms (Prum et al. 1998, Prum 2006, Stavenga et al. 2011, Tinbergen et al. 2013, Shawkey and D'Alba 2017). Avian colouration can have numerous functions, from concealment via cryptic plumage or mimicry to advertising the quality of an individual (reviewed in Bortolotti 2006). In this lattermost context, colour displays may function as signals in mate choice, competition between individuals of the same sex, or parent-offspring communication. However, an important prerequisite of such signalling is signal honesty,

which prevents cheating by lower-quality individuals. According to the condition capture models, the honesty of the signals in the colour patches is ensured by the costs associated with its production and/or maintenance (Zahavi 1977, Grafen 1990). This implies that only individuals in the best condition are able to express and bear the highest quality colour ornaments. For the case of sexually selected traits, another prediction that stems from those models is heightened condition-dependence of colour ornaments in males (reviewed in Cotton et al. 2004).

Despite being built on a firm theoretical framework (Pomiankowski 1987, Grafen 1990), empirical support from well-designed experiments for the condition-dependence model of colour ornaments is still very scarce (Cotton et al. 2004). One notable exception is carotenoid-based colouration, which is unusual in that it cannot be synthesised *de novo* by birds (McGraw 2006).

The underrepresentation of studies investigating condition dependence is especially striking in the case of structurally-coloured ornaments, which – being particularly visually conspicuous – are often the subject of research on sexual selection. Leaving aside white, achromatic feathers (where the colour is produced by even scattering of all wavelengths), bright structural colours are generated by coherent light scattering by keratin nanostructures and melanosomes (Prum et al. 1998, Prum 2006, Wilts et al. 2014, Igic et al. 2016). Such colouration can be divided into iridescent colouration, generated by laminar or crystal-like nanostructures located in the feather barbules, and matte, non-iridescent colouration produced by quasi-ordered spongy-like keratin nanostructures inside the barbs (Prum and Torres 2003). The honesty of structurally-coloured ornaments is thought to be ensured by the costs of keratin and melanin pigment production (Meadows et al., 2012). However, recent histological studies suggested that the growth of spongy nanostructure involves few to no metabolic costs (Shawkey et al. 2006, Prum et al. 2009). To our knowledge, there are no experimental studies examining the proximate mechanisms of condition-dependence of nanostructures, and only a few previous studies addressing relationships between structure and colour variation in general: for iridescent colour in the satin bowerbird (*Ptilonorhynchus violaceus*, Doucet et al., 2006) and for non-iridescent colour in the bluebird (*Sialia sialis*, Shawkey et al., 2003, 2005) the blue tit (*Cyanistes caeruleus*, Hegyi et al. 2018), and in nine species of fairy-wren (Malurus spp.; Fan et al. 2019).

The timing of physiological impacts on feather colour and quality are also unstudied. Some evidence comes from studies on feather renewal processes. The quality of feathers is sensitive to perturbations or stressors during moult in adult birds (e.g. Griggio et al. 2009, Vagasi et al. 2012), and juvenile feathers produced during energetically demanding period of nestlings' growth are even more sensitive to early rearing conditions (Tschirren et al. 2003, Jacot and Kempenaers 2007). During the first days of a nestlings' life, the majority of nutrients are invested in rapid growth and intensive metabolic processes, but also in feather follicle formation. After the feather pins are visible, the internal barb cells continue to mature, so processes important for the development of colour producing structures occur while the feather is growing (Prum 2009). Thus, the question of how early growing conditions affect structural coloration of juvenile feathers can be complemented with a further question: which stage of a nestlings' growth is most important in this process.

Here, we used an experimental brood size manipulation to investigate the influence of early rearing conditions on non-iridescent structural colouration of blue tit nestlings. The blue tit is a widespread cavity-nester that readily breeds in nest-boxes, simplifying the monitoring of nestlings. More importantly, it has contrasting, conspicuous plumage. These features make it a particularly suitable model species for studying colouration in birds. Experimental studies are facilitated by the fact that juvenile blue tits express UV/blue, non-iridescent structural colouration in the tail feathers (Figure 1), with greater expression levels in males (Johnsen et al. 2003). Furthermore, in contrast to the breast feathers that are replaced during the postjuvenile moult, most tail feathers are moulted only after the first breeding season, which means they may play a signalling function both in parent-offspring communication and – beyond the nestling period – in mate choice. Consequently, variation in this particular ornamented trait may be subjected to different selection pressures (Jacot and Kempenaers 2007). Both breast and tail colouration of blue tit nestlings were shown to be condition dependent in correlational (Johnsen et al. 2003) and experimental (Jacot and Kempenaers 2007) studies, but only the latter study showed a sex-specific effect on rectrices structural colouration. A very recent quantitative genetics study, besides finding low heritability of tail structural colouration, surprisingly, showed that, at a genetic level, UV chroma of rectrices is negatively related to the proxies of a bird's performance: body mass, wing length and cell-mediated immunity (Class et al. 2019).

In this study, we used a two-stage brood size manipulation design, with nests enlarged either at an early or late stage of nestlings' growth. Brood size manipulation has been repeatedly

shown to affect nestlings' traits, including body mass, tarsus length, condition, immune response and colouration (e.g. Cichoń and Dubiec 2005, Jacot and Kempenaers 2007). Here, as a criterion for dividing the development of chicks into two phases, we determined that pins of tail feathers begin to appear on the skin surface around the 6th day after hatching. Among the early enlarged nests, one group was reduced back to the original brood size in the second stage of nestlings' growth, while the other remained enlarged. This experimental design allows us to discriminate at which stage of nestlings' growth greater within-nest competition more strongly influences the developing plumage. We predicted that impaired early growth conditions should negatively influence barbs' micro-scale morphology and thus their brightness and UV chroma. We predicted that this effect would be stronger in nestlings from early-enlarged broods, compared to the late-enlarged and control broods. Furthermore, given the sex-specific condition-dependence of tail feathers colouration found by Jacot and Kempenaers (2007), we predicted that the internal structure of male feathers would be significantly different from that of females, and more sensitive to deterioration of early development conditions compared to females.

Materials and methods

Field study

The study was conducted over two field seasons: 2017 and 2018, in a nest-box population of blue tits (*Cyanistes caeruleus*), inhabiting the island of Gotland (Sweden, 57°01'N 18°16'E). The study area is covered with fields and meadows, having patches of deciduous and mixed forests, dominated by oak, *Quercus robur L.* and ash, *Fraxinus excelsior L.*, with an admixture of hawthorn, *Crataegus spp L.* and hazel, *Corylus avellana L.* (see Pärt & Gustafsson 1989 for more detailed description). In this population hatching date may vary between mid-May to the beginning of June, the incubation period lasts two weeks and the majority of nestlings from one nest hatch during a single day, although some degree of hatching asynchrony is observed. Nestlings are fed mainly with caterpillars, less often with mosquitos or spiders and fledge 18-22 days after hatching (Drobniak et al. 2014).

From the end of April, we regularly inspected nest-boxes to track the nest-building process, assess the number of eggs and the beginning of the incubation period. During the incubation, females were not disturbed until the expected hatching date. On the second day after hatching we weighed nestlings, marked them by nail clipping and took a small blood sample from the tarsal vein. On the 8th day after hatching, we ringed and on the 14th weighed, and measured

the tarsus length of nestlings. On day 18, we collected the second right rectrix from each nestling. We regressed the body mass at day 14 against the tarsus length to obtain a measure of mass independent of body size. Further in this manuscript we refer to it as 'residual mass' (in other studies this metric is also called body condition e.g. in Jacot and Kempenaers 2007).

Experimental protocol and sampling

To manipulate nestlings' rearing conditions we performed a two-stage brood size manipulation experiment, with three types of enlarged broods (Figure 2). In the "Early1" group, the brood size was enlarged at day 2 and left without further manipulation until fledging. The second group "Early2" was enlarged at day 2, but donor nestlings were removed at day 6 and transferred to nests from the third group "Late". The fourth group was not manipulated and constituted a control ("Ctrl"). Nests for the experiment were chosen to create blocks of four nests with matched hatching date (±1 day) and number of nestlings (±1 egg), plus one donor nest (not considered in further analyses) with the same hatching date. Both "Early1" and "Early2" groups were enlarged by three randomly chosen chicks from the donor nest. At day 6, when donor nestlings from the group "Early2" were relocated to the group "Late", we visited the nests from the remaining groups as well, to keep the disturbance level equal. We had 6 experimental blocks with a total of 214 nestlings in the first breeding season and in the following season 5 blocks, with 206 nestlings in total (see Table S1 for exact numbers of nestlings in each experimental group).

Feather morphology and colouration

We measured the total length of plucked tail feathers samples (distance from feather tip to the end of the calamus) and the length of the feather sheath of rectrices with a digital calliper to the nearest 0.1 mm. To estimate the degree of feather development, we divided the length of erupted part of feather by the total feather length (hereafter referred to as "development coefficient").

Feather reflectance measurements were performed using an Ocean Optics Maya Flame spectrophotometer (Dunedin, FL, USA) with bifurcated probe 7 × 400μm and a xenon pulsed light source. On each rectrix, we made 10 reflectance measurements along the outer (the most brightly coloured) vane. Obtained spectra were averaged, smoothed and further analysed using the package *pavo* (Maia et al. 2013) in R (version 3.1.2). For spectral analysis we calculated set of reflectance-based colour metrics, among which we chose for further analysis: brightness (total reflectance), UV chroma and red chroma calculated respectively, as the sum

of reflectance values of regions from 300 nm to 400 nm and 605 nm to 700 nm, divided by the total reflectance in the given region (Maia et al. 2013).

Molecular sex assessment

DNA was extracted from blood samples stored in 96% ethanol, using Chelex (Bio-Rad, Munich, Germany) following the manufacturer's protocol (Walsh et al. 1991). Sexing was performed following a well-established PCR-based method (R. Griffiths, M. C. Double, K. Orr 1998).

Scanning Electron Microscopy (SEM)

To compare the internal microstructure morphology of the feather barbs we used scanning electron microscopy (SEM). The order of the nests for SEM preparations was generated randomly and from each experimental nest we randomly chose (by drawing envelopes with samples) 3 nestlings for SEM rectrix preparations. Donor nestlings (in groups Early1 and Late) and feathers with erupted parts shorter than 1 cm were excluded from the analysis. After removing 2-3 mm of the distal tip of a feather, a fragment of the rectrix outer vane was sliced perpendicularly to the barbs, so that the cut-out fragment contained 6 -11 barbs cross-sections. The sectioned fragment was mounted on a graphite block covered with carbon adhesive tape and sputter coated with gold. Samples were viewed on a cold field emission Scanning Electron Microscope (SEM) HITACHI S-4700 at magnifications x1300 and x5000. From each feather, three cross-sections were chosen, excluding the outermost, the one closest to the vane, as well as the ones that were crushed, damaged or contaminated by visible debris. Using the ImageJ software (Rasband 2004), we measured the following characteristics of the barb's microstructure (Figure 4.B): height and width of a cross-section, number and area of air cavities, the area of the medullary part, the cortex area, the total area, total number of melanosomes and melanosome density (D'Alba et al. 2014).

Small angle X-ray scattering (SAXS)

In many previous studies (since the early work of Dyck 1971) feather nanostructures were analysed with transmission electron microscopy (TEM), which gives very precise, high quality images. However, due to the time-consuming preparation and the probability of sample shrinkage this method has some limitation in quantitative studies on bigger sample sizes (Saranathan et al. 2012). Instead, we used small angle X-ray scattering (SAXS) to quantitatively characterize the length-scales of the nanostructures present in the barbs

(Saranathan et al. 2012, Parnell et al. 2015). SAXS analysis allows us to predict the interaction between the incident light and the nanostructure of analysed sample, and therefore predict the optical properties of the feather (Saranathan et al. 2012). In subsequent analysis, we used the following metrics: maximum peak height, peak position, and full-width at half-maximum of the peak (further referred to as FWHM). Maximum peak height relates to the intensity of the scattering of nanostructures and SAXS peak position (in the q domain) is inversely proportional to the wavelength position of the peak reflectance. The FWHM value is a measure of the nanostructure size distribution (short-range quasi-periodic order). Narrow structural peaks with a smaller FWHM mean more defined nanostructure whilst higher values of FWHM indicate a larger spread in length-scales, and thus a broader optical reflectance peak meaning less saturated colours (Saranathan et al. 2012).

The SAXS measurements were performed on a subset of tail feathers from the 2017 season. We excluded samples from donor nestlings and underdeveloped or poor-quality feather samples, which eventually resulted in a sample size of 166 individuals, with equal numbers in experimental groups ($\chi^2 = 0.48$, df = 3, p = 0.92). SAXS measurements were carried out using a Xeuss 2.0 (Xenocs, Grenoble France) SAXS system, with a liquid gallium X-ray source (MetalJet Excillum, Sweden). The feather samples were mounted in an aluminium frame and the measurements were taken from the region of outer vane, located 5 mm below the distal tip of the feather. The X-ray beam (9.24 keV) diameter was 300 µm vertically and 250 µm horizontally, with a distance of 6.5 m between sample and detector (Pilatus3R 1M 2D, Dectris, Switzerland). Each individual feather sample was measured for a period of 180 seconds, with the data being processed using the software Foxtrot 3.3 (Soleil, France), the detector images were masked to account for the detector gridlines and hot pixels, the image was then radially integrated to give the scattered intensity as a function of the scattering wave-vector q (Saranathan et al. 2012). The structural peak from the optical nanostructure in the feathers was measured using the SAXS scattering curve transformed into the Lorentz corrected Iq^2 versus q form, and the structural peak was fitted using a Lorentz peak function.

Statistical analysis

The overall sample size, after excluding all donor nestlings, comprised 420 birds, from 44 experimental nests (Table S1), equally distributed between experimental groups ($\chi^2 = 0.057$, $df = 3$, $p = 0.996$). Due to nestlings fledging before sampling of tail feathers (two whole nests in 2018 and numerous individual cases) or inadequate quality of collected samples, the

sample size for feather colouration was reduced to 334. The sex was assigned for 375 nestlings, with equal sex ratio, confirmed by a Chi-square test ($\chi^2 = 0.45$, $df = 1$, $p = 0.502$).

To test for differences in the survival rate between experimental groups, a generalized linear mixed model with a binomial error was applied with fledging success introduced as the dependent variable, experimental group as a fixed factor and nest as a random term. The effects of experimental treatment on nestlings' residual body mass, tarsus length, tail feather development, colouration, microstructure and nanostructure characteristics, were analysed using a general linear mixed effect model. The models included experimental treatment, nestling sex and year as fixed explanatory variables and nest of rearing defined as a random term. In all analyses we first tested for the interaction between experimental treatment and sex of the nestlings, but wherever this interaction was not significant it was removed from the models.

Since some of the characteristics obtained from SEM images might be interdependent, a principal component analysis (PCA) was used to summarize barb microstructure variables. We extracted the first two principal components explaining 59.95% and 18.43 % of variance, respectively, which were used as dependent variables in further analysis (see Figure 6 for biplot of PC1 and PC2). PC1 had very strong negative loadings for total area of cross-section (-0.97) and area of medullary part (-0.96), medium negative loadings for the rest of keratin-based variables (Table S2), and medium (-0.63) and low (-0.25) loading respectively for, the number and density of melanosomes. Thus, PC1 described the size and internal structure of barbules, with higher values of PC1 signifying thinner, flatter barbules with less cortex and medullar keratin. PC2 described mainly variation in melanin-based component with negative factor loading for number and density of melanosomes (-0.76 and -0.95; Table S2). Thus, PC2 could be interpreted as a melanosome scarcity parameter: higher values indicating lower numbers of melanosomes. The first two PC components were further used as dependent variables in subsequent analysis. In those two models, to account for potential differences between the cross-section resulting from the distance from the rachis, the numbered order of a cross-section was introduced as an additional explanatory variable in the analysis. Because we analysed three cross-sections per individual, the individual identity was introduced as another random term. All analyses were performed in R using the '*lme4*' and '*lmerTest*' packages for linear mixed models, '*factoextra*' for PCA analysis and '*ggplot2*' for graphs (R Core Team).

Results

283 *Nestlings body mass, tarsus length and fledging success*

284 Experimental treatment negatively affected nestlings residual body mass at day 14 in the
285 Early1 group and positively in Early 2 group (Table 1). Tarsus length was not affected by
286 experimental manipulation in any of the groups (Table 1). For both residual mass and tarsus
287 length, the interaction between experimental treatment and nestlings sex was not significant in
288 any of the groups. There was no difference in nestlings fledging success between
289 experimental groups (data not shown) and the average fledging success was 87.17%.

290 *Tail feathers development and colouration*

291 Tail feathers were significantly shorter in chicks of enlarged broods, and this effect was more
292 marked among males. (Table 1, Figure 3.C). This pattern was even stronger for the rectrix
293 coefficient of development, where interaction with sex appeared significant also in the Early2
294 group, with the same effect direction (Table 1). Contrary to predictions, colour metrics of tail
295 feathers were not significantly affected by experimental manipulation (Table 2, Table S3).
296 However, there was a close-to significant trend of lower UV chroma in the "Late" group.
297 Independently of experimental manipulation, UV chroma was significantly higher in males
298 (Table 2.B, Figure 5.A), while red chroma was higher in females (Table S3.) The mean and
299 standard deviation values of nestling mass, tarsus length, tail feather parameters and colour
300 metrics, averaged within experimental group and sex are given in Table S4.A and S5.A,
301 respectively.

302 *Micro- and nano-structure characteristics of tail feathers*

303 SEM images of barb's rami cross-sections revealed a medullary area consisting of dead
304 keratinocytes containing channel-type ß-keratin spongy nanostructure with interspersed
305 melanosomes and centrally located air cavities (Figure 4.A). Nestlings from late enlarged
306 broods had smaller diameters of barb's keratin morphological elements (PC1, Table 3, Figure
307 S1.A), while other groups did not differ from the control. Number and density of
308 melanosomes (PC2) did not differ between groups (Table 3, Figure S1.B). In both models
309 with PC components, there were differences between sexes, with males having wider and
310 thicker barbs, larger medullary area, more air vacuoles, and tended to have more
311 melanosomes relative to female chicks (Table 3). The means and standard deviations of tail
312 feather barb cross-section microstructure variables, averaged within experimental group or
313 sex are given in Tables S4.B and S5.B, respectively.

None of the quantitative SAXS metrics (maximum peak height, peak position, nor FWHM) were affected by experimental manipulation (Table 4), however for the FWHM, the estimate in the Late group was an order of magnitude higher than in both early enlarged groups. The interaction between experimental treatment and sex of the nestlings was not significant in any of the models, though there were significant differences in all three SAXS metrics between males and females (Figure 5.B and C). This means that male keratin nanostructure generate shorter-wavelength reflectance peaks (according to the position of the SAXS peak in q space), have stronger scattering keratin nanostructures (according to the intensity of the SAXS scattering) and – most importantly – are characterised by more regular structure than females (according to the FWHM parameter) (Table 4). The means and standard deviations of tail feather of Small angle X-ray scattering (SAXS) metrics, averaged within experimental group or sex are given in Tables S4.C and S5.C, respectively.

Discussion

The experimental treatment significantly affected residual body mass in both of the early enlarged groups, however, only in the group that remained enlarged was the effect negative as predicted (Table2, Figure 3.A). Nestlings from the "Early2" group, with broods enlarged only during the first days of early growth, unexpectedly turned out to be heavier, and this effect was consistent for both experimental seasons. Late enlargement of the brood did not change nestlings' body mass. However, interestingly, in this group we observed a sex specific rectrix development delay, with males being more sensitive to the experimental manipulation than females (Table2, Figure 3.C). An analogous pattern, but with smaller effect size, was present in the "Early2" group. Therefore, the effect of the experimental manipulation on the parameters connected with general condition was different for each of the experimental groups.

Contrary to predictions, neither brightness, nor UV chroma of tail feathers was affected in any of the experimental groups. The only detectable tendency was a non-significant decrease of UV chroma in the "Late" group, with an estimated similar order of magnitude as the increase in UV chroma in males relative to females. Accordingly, in the study with brood size manipulation of Jacot and Kemepenaers (2007) blue tit nestlings from enlarged nests did not differ from the controls with regard to brightness and UV chroma of tail feathers. However, in their study, males raised in reduced broods developed feathers with higher UV chroma. This sex-specific effect was hypothesised to be the result of early-acting sexual selection, as tail

346 feathers are not replaced during post-juvenile moult, and this was hypothesised to play a
347 signalling role in mate choice during the first breeding season (Jacot and Kemepenaers 2007,
348 Class et al. 2019, Badass et al. 2020). Interestingly, in a brood size manipulation experiment
349 on eastern bluebirds (*Sialia sialis*), structurally coloured wing feathers were also shown to be
350 brighter in male nestlings from reduced broods, compared to those from enlarged broods,
351 while no analogous effect was found in females (Siefferman and Hill 2007). In accordance
352 with our results, manipulation of early rearing conditions did not change feathers' UV
353 chroma, although in both cases it was significantly higher in males. It seems important that in
354 the above published studies, observed effects appeared for males in reduced broods, i.e. in
355 improved early growing conditions, while brood size enlargement did not produce a
356 symmetrical negative effect. It is possible that in our study the colour difference was obscured
357 by the difficulty of accurately measuring the colour of very thin and narrow outer vanes of
358 freshly developed nestling rectrices. Thus, we have tried to explore possible underlying colour
359 moderators, looking at the nano- and micro-scale characteristics of the assayed feathers.

360 In non-iridescent UV-blue feather colour, hue and UV chroma in particular, depend on the
361 arrangement of nano-scale keratin structures in the medullary part of the feather barb (Prum
362 1998, Shawkey et al. 2005). We found significant sex differences, with males having higher
363 values of all three SAXS metrics (Figure 5.B and C). Most importantly, males exhibited
364 higher q value centred peaks, which indicates smaller short-range quasi-periodic order of
365 nanostructure (Saranathan et al. 2012), and hence shorter wavelength of peak reflectance
366 (shifted towards UV), which explains dichromatism in UV chroma. These results emphasize
367 that the SAXS method detects patterns complementary to spectrophotometric predictions,
368 even in relatively thin, finely coloured and freshly developed feathers such as those used in
369 our study. Nevertheless, contrary to predictions, we found no differences in the SAXS
370 morphometrics between experimental groups. Perhaps this low sensitivity of spongy structure
371 to manipulated early growing conditions, might be explained by the likelihood that
372 nanostructures in the medullary cells are produced via self-assembly in a process called
373 spinodal decomposition that does not require significant energy input or, limiting nutrients
374 (Prum et al. 2009).

375 However, other microstructural elements of barb morphology and their characteristics are also
376 critical to the mechanism of colour production (Fan et al. 2019). At the micro-scale we found
377 that barb characteristics were impaired in late-enlarged broods. Width of barb cross-section,
378 total area, medullary area, vacuoles number and area all decreased, while the density of

melanosomes was not affected (although we noted a very close to significant trend of lower melanosome numbers in the "Late" group, Table 3). This is only a partial confirmation of our expectations, because we predicted an analogous, but more strongly pronounced, effect in both early enlarged groups. We must note that SEM imaging is not an optimal method for measuring melanosomes density (due to low contrast, making discrimination between morphological features difficult) and we treat this parameter more as an approximation than an exact value. However, the pattern we obtained for group "Late" shows some similarity to D'Alba et al. (2014), examining condition dependence of melanin-based colouration in zebra finches (*Taeniopygia guttata*) exposed to unpredictable food supply during development and black-capped chickadees (*Poecile atricapillus*) affected by avian keratin disorder. In both cases, the density of melanosomes did not differ between control and experimental groups, while barbule density (keratin component) was consistently higher in controls (D'Alba et al. 2014). This can be explained by the fact that melanin is endogenously synthesised (McGraw 2006), and currently there is no evidence that would indicate that it is expensive to produce.

We predicted that the negative effect of impaired early growth conditions on feather structure and colouration would be more pronounced in nestlings from early-enlarged broods, compared to late-enlarged and control broods. However, in terms of feather development and microstructure, the most sensitive to manipulation was the "Late" group. This suggests that the current availability of resources has a greater effect on feather development than current body condition, which could be determined at earlier stage of nestling growth. Previous experimental studies, with accelerated moult rate in adult birds, demonstrated that feather quality is sensitive to perturbations during feather development (e.g. Griggio et al. 2009, Vagasi et al. 2012). On the other hand, it is also possible that the smaller barb diameters were caused by the slowdown of tail feather development, as feathers from this group were also shown to be shorter. Our sampling (18^{th} day) took place before the completion of the bottom feather portion growth, thus we have no data on the final achieved tail feather length. Unfortunately, sampling of young birds in the period between the fledging and the next breeding season is virtually impossible.

We predicted that feather structure would differ between males and females, and that males would be more sensitive to the manipulation of early growing conditions. Indeed, sex differences were present at all levels of feather structure: from the length of rectrices, through the micro-scale parameters of barbs, to the nanoscale characteristics, described by SAXS metrics. However, feather colour did not vary in relation to brood enlargement. Within the

optical properties, we found that beside the UV region, with reflectance higher in males, significant differences are also present at long-wavelengths, except that in this region higher reflectance occurs in females. According to Fan et al. (2019), reflectance at long wavelengths might depend on the spatial frequency and thickness of spongy layer and cortex. Perhaps then, higher reflectance in the long-wavelength region in females results from the larger nanostructure of the spongy structures in females feathers (as suggested by the larger values of both SAXS peak position and FHWM in females, Saranathan et al. 2012). To a certain extent, reflectance at long wavelengths might be also affected by the density of melanosomes, which is higher in males, however, absorption properties of melanin decline with increasing wavelength (Xiao et al. 2018), therefore this factor may have only a limited effect.

Finally, nestlings from the "Early2" group (where broods were enlarged during first days of development, but reduced at day 6) had higher residual body mass, consistently in both of the study seasons. This unexpected result suggests that the amount of parental investment might be fixed at a very early stage of offspring development. Alternatively, the first stage of nestling development might be less costly for parents – but in this scenario, the negative effect of similar strength in the "Late" group as in "Early1", but this was not the case. We suggest a potential future study with similar experimental design, but controlling for parental effort (feeding frequency, quality of food brought to nest), is needed.

To conclude, our results suggest that, contrary to carotenoid-based colouration (which in tits was proposed to be largely determined by the amount of carotenoids deposited to egg yolk and the feeding during the first six days (Fitza et al. 2003)), feathers with structural colouration are more sensitive to conditions experienced during feather growth in the later phases of nesting period. We demonstrated that the quality of the spongy ß–keratin nanostructure in the blue tit tail feather's barbs does not appear to be sensitive to early rearing conditions. However, other keratin components of barb morphology, like the medullary layer area in a barb or the number of air vacuoles seem to be more sensitive to perturbation during early development. To our knowledge, this is the first experimental study were SAXS and SEM analysis were applied to quantitatively examine the quality of structural colouration, and the first study that looked at inter-sexual differences in these parameters. Future studies should focus on elucidating the mechanism mediating condition-dependence and sexual dichromatism in structurally coloured ornaments.

Acknowledgements

We are very grateful to Marek Michalik for consent for carrying out the SEM analysis in the Laboratory of Scanning Microscopy in the Institute of Geological Sciences in Jagiellonian University, and to Olga Woźnicka and Grzegorz Tylko for introducing K.J. to electron microscopy. We are very grateful to Liliana D'Alba, Bram Vanthournout and other members of Evolution and Optics of Nanostructures Group, of University of Ghent, and Agnieszka Gudowska of the Institute of Environmental Sciences, Jagiellonian University, for very helpful and constructive comments on the previous version of the manuscript. We thank Johan Träff for providing nestlings photographs, as well as Magda Zagalska-Neubauer and Tomasz Kowalczyk for their assistance in the fieldwork.

Competing interests

The authors declare no competing or financial interests.

Author contributions

Conceptualization: K.J., S.M.D., M.D.S, M.C.; Methodology: K.J., M.D.S, S.M.D., A.P.; Validation: S.M.D.; Formal analysis: K.J., S.M.D.; Investigation: K.J., A.Ł., D.L., J.B., A.P., S.M.D.; Resources: K.J., A.Ł., S.M.D., A.P. L.G.; Data curation: K.J., S.M.D., A.P.; Writing - original draft: K.J.; Writing - review & editing: D.L., A.P., M.D.S, A.Ł., L.G., J.B., M.C., S.M.D.; Visualization: K.J., A.P; Supervision: S.M.D, M.C.; Project administration: K.J; Funding acquisition: K.J., S.M.D., M.D.S.

Funding

This study was financed by the National Science Centre: to K.J., grant no. UMO-2015/19/N/NZ8/00404 and to S.M.D grant no. UMO-2015/18/E/NZ8/00505, and by the Fonds Wettenschapelijk Onderzoek G007117N to M.D.S.

Data availability

Authors declare to deposit data to the Dryad Digital Repository.

References

Badás, E., Autor, A., Martínez, J., Rivero-de Aguilar, J. and Merino, S. 2020. Individual quality and extra-pair paternity in the blue tit: sexy males bear the costs. Evolution. Accepted Author Manuscript. doi:10.1111/evo.13925

Bortolotti G. R.. 2006. Natural selection and avian coloration: protection, concealment, advertisement or deception? Chapter 1. *in* Bird coloration: Volume 2: function and evolution. (G.E. Hill and K.J. McGraw, eds.) Harvard University Press. pp. 3-35.

475 Drobniak S.M., Dubiec A., Gustafsson L., Cichoń M. 2014. Maternal Age-Related Depletion
476 of Offspring Genetic Variance in Immune Response to Phytohaemagglutinin in the Blue Tit
477 (*Cyanistes caeruleus*). *Evol Biol*. 42(1): 88-98.

478 Cichoń, M. and Dubiec, A. 2005, Cell-mediated immunity predicts the probability of local
479 recruitment in nestling blue tits. J. Evol Biol, 18: 962-966.

480 Class, B, Kluen, E, Brommer, JE. 2019. Tail colour signals performance in blue tit nestlings. J
481 Evol Biol.; 00: 1– 8.

482 Cotton S, Fowler K, Pomiankowsi A. 2004. Do sexual ornaments show heightened condition-
483 dependent expression as predicted by the handicap hypothesis? Proc R Soc Lond B. 271:771–
484 783.

485 D'Alba L., Van Hemert C., Spencer K. A., Heidinger B. J., Gill L., Evans N. P., Monaghan
486 P., Handel C. M., Shawkey M. D., 2014. Melanin-Based Color of Plumage: Role of Condition
487 and of Feathers' Microstructure. Integr. Comp. Biol. 54: 633–644.

488 Doucet, S. M., Shawkey, M. D., Hill, G. E., and Montgomerie, R. 2006. Iridescent plumage in
489 satin bowerbirds: structure, mechanisms, and nanostructural predictors of individual variation
490 in colour. J Exp Biol 209: 380-390.

491 Dyck, J. 1971. Structure and spectral reflectance of green and blue feathers of the rose-faced
492 lovebird (*Agapornis roseicollis*).- Dansk. Vid. Selsk. Biol. Skr. 18: 1-67.

493 Fan M., D'Alba L., Shawkey M. D, Peters A., Delhey K. 2019. Multiple components of
494 feather microstructure contribute to structural plumage colour diversity in fairy-wrens, Biol. J.
495 Linnean. Soc. 128, 550–568. https://doi.org/10.1093/biolinnean/blz114

496 Fitze, P.S., Tschirren, B. & Richner, H. 2003. Carotenoid-based colour expression is
497 determined early in nestling life. Oecologia 137: 148–152.

498 Grafen, A. 1990. Biological signals as handicaps. Journal of Theoretical Biology 144:517–
499 546.

500 Griffiths, R., Double, M., Orr, K. & Dawson, R. 1998. A DNA test to sex most birds. Mol.
501 Ecol. 7: 1071–1075.

502 Griggio, M., Serra, L., Licheri, D., Campomori, C. and Pilastro, A. 2009. Moult speed

503 affects structural feather ornaments in the blue tit. J. Evol. Biol. 22, 782-792.

504 Hegyi G., Laczi M., Kötél D., Csizmadia T., Lőw P., Rosivall B., Szöllősi E., Török J. 2018.
505 Reflectance variation in the blue tit crown in relation to feather structure. J Exp Biol 221, doi:
506 10.1242/jeb.176727.

507 Henderson, L.J., Heidinger, B.J., Evans, N.P. and Arnold, K.E. 2013. Ultraviolet crown

508 coloration in female blue tits predicts reproductive success and baseline corticosterone.

509 Behav. Ecol. 24, 1299-1305.

510 Hill, G. E. 1992. Proximate basis of variation in carotenoid pigmentation in male house
511 finches. Auk 109:1–12.

512 Igic B., D'Alba L., Shawkey M. D. 2016. J. Exp. Biol. Manakins can produce iridescent and
513 bright feather colours without melanosomes 219: 1851-1859.

514 Jakob E. M., Marshall S. D., Uetz G. W. 1996. Estimating fitness: a comparison of body
515 condition indices. OIKOS 77: 61-67

516 Jacot, A., Kempenaers, B. 2007. Effects of nestling condition on UV plumage traits in blue
517 tits: an experimental approach. – Behav Ecol. 18: 34–40.

518 Jacot, A., Romero-Diaz, C., Tschirren, B. Richner, H., Fitze, P.S. 2010. Dissecting carotenoid
519 from structural components of carotenoid-based coloration: a field experiment with Great tits
520 (*Parus major*). – Am. Nat. 176: 55–62.

521 Johnsen, A., Delhey, K., Andersson, S., & Kempenaers, B. 2003. Plumage colour in nestling
522 blue tits : sexual dichromatism, condition dependence and genetic effects. Proc. R. Soc. Lond.
523 B Biol Sci., 270, 1263–1270.

524 Maia, R., Eliason, C.M., Bitton, P. P., Doucet, S.M. and Shawkey, M.D. 2013. pavo: an R
525 Package for the analysis, visualization and organization of spectral data. – Method Ecol. Evol.
526 4(10): 609-613.

527 McGraw, K. J., and G. E. Hill. 2001. Carotenoid access and intraspecific variation in plumage
528 pigmentation in male American goldfinches (*Carduelis tristis*) and northern cardinals
529 (*Cardinalis cardinalis*). Funct. Ecol. 15:732–739.

530 McGraw K. J. 2006. Mechanics of Carotenoid-Based Coloration. Chapter 5. in Bird
531 coloration: Volume 1: Mechanisms and measurements. (G.E. Hill and K.J. McGraw, eds.)
532 Harvard University Press. pp. 177-242.

McGraw K. J. 2006. Mechanics of Melanin-Based Coloration. Chapter 6. *in* Bird coloration: Volume 1: Mechanisms and measurements. (G.E. Hill and K.J. McGraw, eds.) Harvard University Press. pp. 243-294.

Meadows, M.G., Roudybush, T.E. and McGraw, K.J. 2012. Dietary protein level affects iridescent coloration in Anna's hummingbirds, *Calypte anna*. J. Exp. Biol. 215, 2742-2750.

Møller, A.P., Biard, C., Blount, J.D., Houston, D.C., Ninni, P., Saino, N. & Surai, P.F. 2000. Carotenoid-dependant signals: indicators of foraging efficiency, immunocompetence or detoxification ability? Avian Poultry Biol. Rev. 11: 137–159.

Pärt, Y. & Gustafsson, L. 1989. Breeding dispersal in the Collared Flycatcher (*Ficedula albicollis*): possible causes and reproductive consequences. J. Anim. Ecol. 58: 305 – 320.

Parnell, A. J. et al. 2015. Spatially modulated structural colour in bird feathers. Sci. Rep. 5, 18317; doi: 10.1038/srep18317.

Pomiankowski, A. 1987 Sexual selection: the handicap principle does work—sometimes. Proc. R. Soc. Lond. B 231, 123–145.

Prum, R. O., Torres, R. H., Williamson, S., & Dyck, J. 1998. Coherent light scattering by blue feather barbs. Nature, 396(6706), 28–29.

Prum R.O, Torres R.H. 2003. A Fourier tool for the analysis of coherent light scattering by bio-optical nanostructures. Integr Comp Biol. 43:591-602.

Prum, R. O. 2006. Anatomy, Physics and Evolution of Structural Colors. Chapter 7. *in* Bird coloration: Volume 1: Mechanisms and measurements. (G.E. Hill and K.J. McGraw, eds.) Harvard University Press. pp. 295-353.

Prum, R.O., Dufresne, E.R., Quinn, T. and Waters, K. 2009. Development of colour producing β-keratin nanostructures in avian feather barbs. J. R. Soc. Interface 6, S253-S265.

Rasband W. 2004. ImageJ. Bethesda (MD): National Institutes of Health.

R Core Team 2014. R: A Language and Environment for Statistical Computing. Vienna: R Foundation for Statistical Computing. Available at: http://www.R-project.org/.

Saranathan, V., Forster J. D., Noh H., Liew S-F., Mochrie S. G. J., Cao H., Dufresne E. R., Prum R. O. 2012. Structure and optical function of amorphous photonic nanostructures from

561 avian feather barbs: a comparative small angle X-ray scattering (SAXS) analysis of 230 bird
562 species. J. R. Soc. Interface 9: 2563–2580.

563 Shawkey M.D., Estes A. M. Siefferman L. M., Hill G. E. 2003. Nanostructure predicts
564 intraspecific variation in ultraviolet–blue plumage colour. Proc. R. Soc. Lond. B. 2701455–
565 1460.

566 Shawkey M. D., Estes A. M., Siefferman L. M., Hill G. E. 2005. The anatomical basis for
567 sexual dichromatism in non-iridescent ultraviolet-blue colouration of feathers. Biol J Linn Soc
568 84:259–271.

569 Shawkey M. D, Hill G.E., McGraw K. J., Hood W.R. and Huggins K. 2006. An experimental
570 test of the contributions and condition dependence of microstructure and carotenoids in
571 yellow plumage coloration. Proc. R. Soc. B 273, doi.org/10.1098/rspb.2006.3675.

572 Shawkey M.D. and D'Alba L. 2017. Interactions between color-producing mechanisms and
573 their effects on the integumentary color palette. Philosophical Transactions of the Royal
574 Society of London B 372: 20160536.

575 Siefferman, L. and Hill, G.E. 2005. Evidence for sexual selection on structural plumage
576 coloration in female eastern bluebirds (*Sialia sialis*). Evolution 59, 1819-1828.

577 Siefferman, L. and Hill, G.E. 2007. The effect of rearing environment on blue structural
578 coloration of eastern bluebirds (*Sialia sialis*). Behav. Ecol. Sociobiol. 61, 1839-1846.

579 Stavenga D. G., Tinbergen J. H., Leertouwer L., B. D. Wilts. 2011. Kingfisher feathers –
580 colouration by pigments, spongy nanostructures and thin films. J. Exp. Biol. 214: 3960-3967 .

581 Tinbergen J., Wilts B. D., Stavenga D. G. 2013. Spectral tuning of Amazon parrot feather
582 coloration by psittacofulvin pigments and spongy structures. J. Exp. Biol. 216: 4358-4364.

583 Tschirren, B., Fitze, P.S. & Richner, H. 2003. Sexual dimorphism in susceptibility to parasites
584 and cell-mediated immunity in Great Tit nestlings. J. Anim. Ecol. 5: 839 – 845.

585 Vagasi C.I., Pap P.L., Vincze O., Benko Z., Marton A., Barta Z. 2012. Haste makes waste but
586 condition matters: molt rate – feather quality trade-off in a sedentary songbird. PLoS One
587 7:e40651.

588 Wilts, B. D., Michielsen, K., De Raedt, H., & Stavenga, D. G. 2014. Sparkling feather
589 reflections of a bird-of-paradise explained by finite-difference time-domain modeling. P.
590 NATL. ACAD. SCI. USA, 111 (12): 4363-4368.

591 Zahavi A. 1977. Cost of honesty—(further remarks on handicap principle). J Theor Biol.
592 67:603–605.

593 Xiao M, Chen W, Li W, Zhao J, Hong Y, Nishiyama Y, Miyoshi T, Shawkey MD,
594 Dhinojwala A. 2018. Elucidation of the hierarchical structure of natural eumelanins. Journal
595 of the Royal Society, Interface 15: 20180045.

596

597 **Tables**

598 **Table 1.** Results of the linear mixed models showing effects of experimental double-stage
599 brood size manipulation on nestlings residual mass, tarsus length and development of tail
600 feathers. The model included experimental group, year and sex as fixed factors and nest of
601 rearing as a random term. Reference levels for fixed effects: exp. group – CONTROL; sex –
602 female; year – 2017.

	Estimate	SE	df	t	p	
Residual mass						
Intercept	959.606	317.040	37.270	3.027	0.004	**
Exp. group (EARLY1)	-0.592	0.220	36.453	-2.695	0.011	*
Exp. group (EARLY2)	0.620	0.227	37.122	2.735	0.010	**
Exp. group (LATE)	-0.111	0.220	36.328	-0.507	0.615	
Sex (Male)	0.080	0.064	326.759	1.247	0.213	
Year (2018)	-0.476	0.157	37.269	-3.027	0.004	**
Tarsus length						
Intercept	-359.151	312.465	36.686	-1.149	0.258	
Exp. group (EARLY1)	-0.305	0.217	36.315	-1.404	0.169	
Exp. group (EARLY2)	-0.027	0.224	36.757	-0.121	0.904	
Exp. group (LATE)	0.011	0.217	36.270	0.051	0.960	
Sex (Male)	0.441	0.041	320.401	10.722	p<0.001	***
Year (2018)	0.186	0.155	36.685	1.203	0.237	
Rectrix lenght						
Intercept	-3682.806	2272.514	36.632	-1.621	0.114	
Exp. group (EARLY1)	-1.441	1.636	38.911	-0.881	0.384	
Exp. group (EARLY2)	2.608	1.594	39.073	1.636	0.110	
Exp. group (LATE)	1.118	1.586	38.378	0.705	0.485	
Sex (Male)	1.734	0.503	277.039	3.448	0.001	***
Year (2018)	1.841	1.126	36.632	1.634	0.111	

Exp. group (EARLY1) : Sex (Male)	-0.522	0.764	277.776	-0.683	0.495	
Exp. group (EARLY2) : Sex (Male)	-1.068	0.745	278.773	-1.433	0.153	
Exp. group (LATE): Sex (Male)	-2.095	0.714	277.575	-2.935	0.004	**
Erupted part						
Intercept	-4180.363	2238.893	34.091	-1.867	0.071	
Exp. group (EARLY1)	-1.028	1.625	39.528	-0.633	0.531	
Exp. group (EARLY2)	1.870	1.583	39.665	1.181	0.245	
Exp. group (LATE)	0.934	1.574	38.866	0.594	0.556	
Sex (Male)	1.035	0.559	276.369	1.851	0.065	
Year (2018)	2.081	1.110	34.090	1.875	0.069	
Exp. group (EARLY1) : Sex (Male)	-0.485	0.846	277.314	-0.573	0.567	
Exp. group (EARLY2) : Sex (Male)	-1.413	0.825	278.476	-1.712	0.088	
Exp. group (LATE): Sex (Male)	-2.629	0.791	277.086	-3.323	0.001	**
Rectrix coefficient						
Intercept	-75.919	42.454	32.647	-1.788	0.083	
Exp. group (EARLY1)	0.013	0.031	41.803	0.408	0.686	
Exp. group (EARLY2)	0.037	0.031	41.768	1.191	0.240	
Exp. group (LATE)	0.035	0.030	40.738	1.149	0.257	
Sex (Male)	0.023	0.013	279.388	1.757	0.080	
Year (2018)	0.038	0.021	32.646	1.801	0.081	
Exp. group (EARLY1) : Sex (Male)	-0.026	0.020	280.739	-1.282	0.201	
Exp. group (EARLY2) : Sex (Male)	-0.044	0.020	282.234	-2.220	0.027	*
Exp. group (LATE): Sex (Male)	-0.070	0.019	280.502	-3.670	p<0.001	***

Table 2. Results of the linear mixed models showing effects of experimental double-stage brood size manipulation on nestlings tail feathers colour metrics. The model included experimental group and the sex as fixed factors and the nest of rearing as a random term. Reference levels for fixed effects: exp. group – CONTROL; sex – female; year – 2017.

	Estimate	SE	df	t	p	
Brightness						
Intercept	586303.900	317823.780	35.420	1.845	0.074	
Exp. group (EARLY1)	34.340	222.260	35.490	0.155	0.878	
Exp. group (EARLY2)	-132.230	217.350	35.950	-0.608	0.547	
Exp. group (LATE)	-97.610	213.620	33.960	-0.457	0.651	
Sex (Male)	-78.510	68.390	273.470	-1.148	0.252	
Year (2018)	-288.290	157.540	35.420	-1.830	0.076	
UV chroma						
Intercept	5.592	8.554	32.680	0.654	0.518	
Exp. group (EARLY1)	0.001	0.006	32.710	0.139	0.890	
Exp. group (EARLY2)	-0.001	0.006	33.140	-0.090	0.929	
Exp. group (LATE)	-0.009	0.006	31.300	-1.544	0.133	
Sex (Male)	0.015	0.002	271.300	8.120	p<0.001	***
Year (2018)	-0.003	0.004	32.680	-0.622	0.538	

608

609 **Table 3**. Results of the linear mixed models showing effects of experimental double-stage
610 brood size manipulation on tail feather barb cross-section microstructure characteristics,
611 expressed as the PC components. Reference levels for fixed effects: exp. group – CONTROL;
612 sex – female; year – 2017; cross-section – 2.

	Estimate	SE	df	t	p	
PC1						
Intercept	-1890.000	1057.000	34.710	-1.788	0.083	
Exp. group (EARLY1)	1.119	0.739	37.520	1.514	0.138	
Exp. group (EARLY2)	0.564	0.713	36.760	0.791	0.434	
Exp. group (LATE)	1.823	0.708	35.830	2.576	0.014	*
Sex (Male)	-1.269	0.349	101.200	-3.634	0.000	***
Year (2018)	0.938	0.524	34.710	1.790	0.082	
cross-section	-0.371	0.031	240.500	-11.803	p<0.001	***
PC2						
Intercept	-882.484	478.699	35.331	-1.844	0.074	
Exp. group (EARLY1)	-0.443	0.333	34.745	-1.331	0.192	
Exp. group (EARLY2)	-0.450	0.321	34.185	-1.404	0.169	
Exp. group (LATE)	-0.539	0.316	32.712	-1.704	0.098	
Sex (Male)	-0.479	0.196	106.236	-2.448	0.016	*
Year (2018)	0.438	0.237	35.334	1.847	0.073	
cross-section	-0.184	0.034	286.622	-5.351	p<0.001	***

613

614 **Table 4.** Results of the linear mixed models showing effects of experimental double-stage
615 brood size manipulation on tail feathers nanostructure SAXS metrics. The model included
616 experimental group and the sex as a fixed factors and the nest of rearing as a random term.
617 Reference levels for fixed effects: exp. group – CONTROL; sex – female.

618

	Estimate	SE	df	t	p	
maximum peak height[1]						
Intercept	1.076	0.143	18.953	7.545	4.02E-07	***
Exp. group (EARLY1)	-0.240	0.208	17.617	-1.156	0.263	
Exp. group (EARLY2)	-0.002	0.209	18.096	-0.012	0.991	
Exp. group (LATE)	-0.270	0.199	17.846	-1.357	0.192	
Sex (Male)	0.097	0.038	126.777	2.537	0.012	*
peak position						
Intercept	2.90E-03	4.84E-05	2.33E+01	59.975	< 2e-16	***
Exp. group (EARLY1)	2.80E-06	6.65E-05	1.74E+01	0.042	0.967	
Exp. group (EARLY2)	6.00E-05	6.82E-05	1.87E+01	0.88	0.39	
Exp. group (LATE)	-2.32E-05	6.42E-05	1.81E+01	-0.361	0.722	
Sex (Male)	2.06E-04	2.57E-05	1.33E+02	8.033	4.58E-13	***
Peak FWHM						

Intercept	3.10E-03	8.34E-05	2.24E+01	37.131	<2e-16	***
Exp. group (EARLY1)	3.87E-05	1.14E-04	1.62E+01	0.340	0.738	
Exp. group (EARLY2)	-4.62E-05	1.17E-04	1.74E+01	-0.395	0.697	
Exp. group (LATE)	1.30E-04	1.10E-04	1.69E+01	1.186	0.252	
Sex (Male)	9.88E-05	4.65E-05	1.33E+02	2.126	0.035	*

[1]coded variable

Figures

Figure 1. Eighteen-day old blue tit nestlings inside the nest-box.

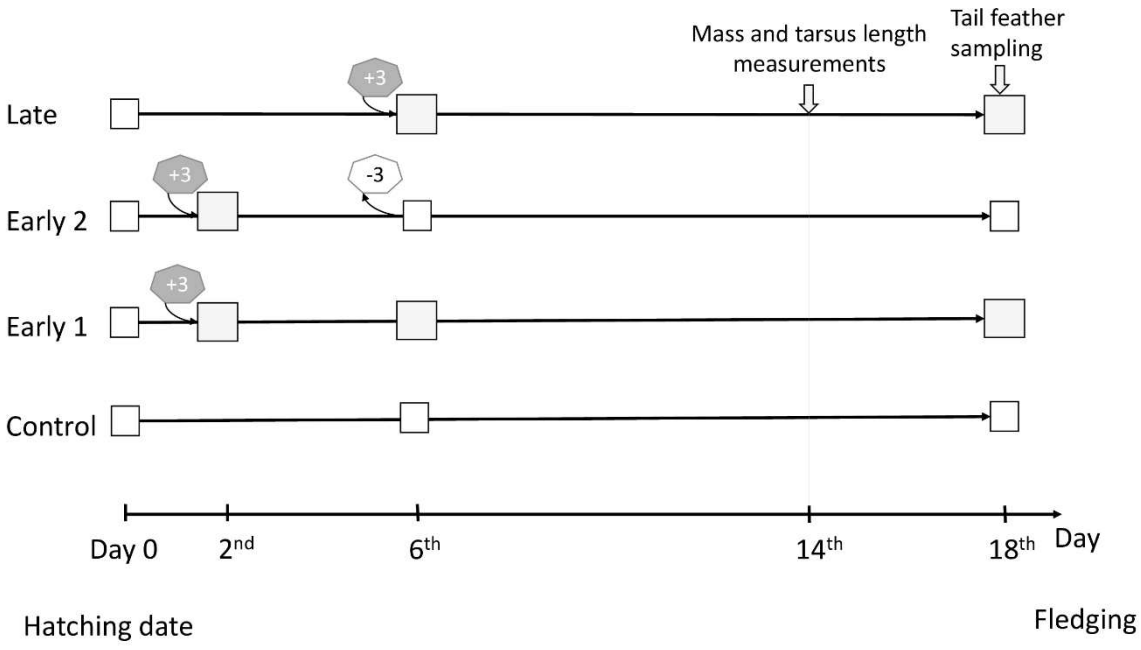

Figure 2. The experimental design scheme for two-stage brood size manipulation.

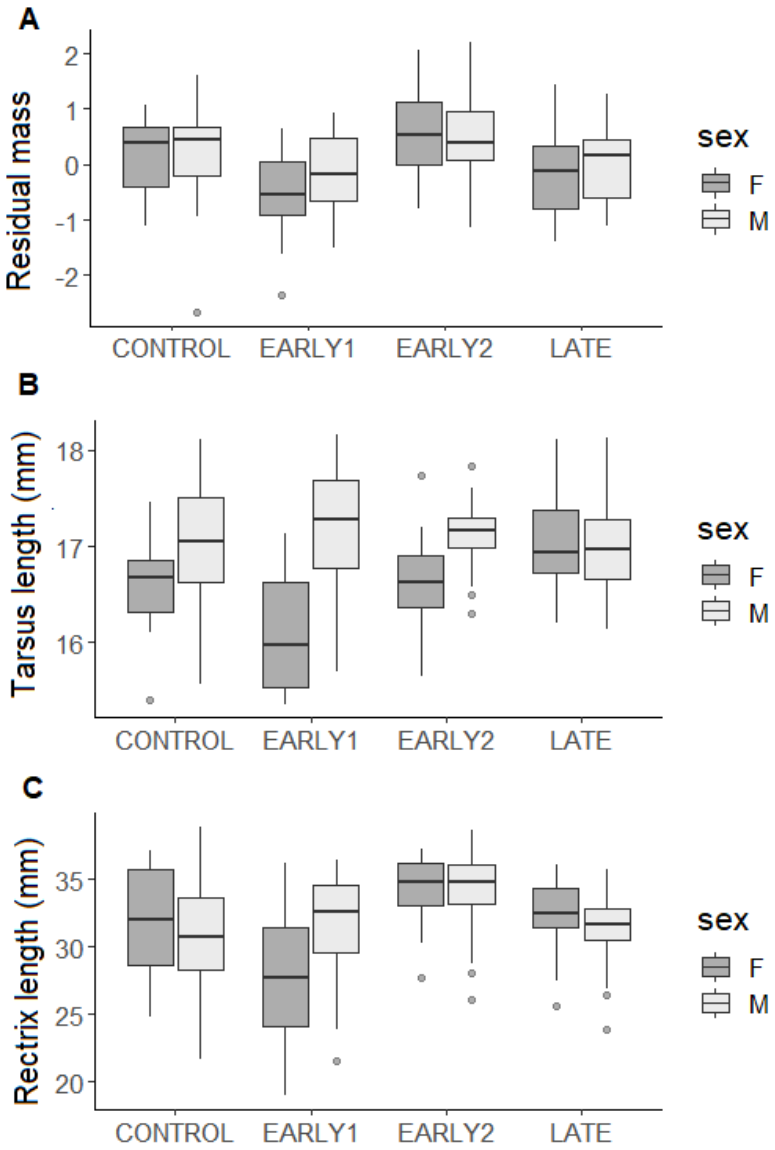

626

627 **Figure 3.** Differences in residual mass (A), tarsus length (B) and rectrix length (C) between
628 experimental groups. "Early1" indicates the group in which broods were enlarged at day 2
629 and left without further manipulation until fledging, in the group "Early2" broods were
630 enlarged at day 2, and subsequently reduced at day 6, in the group "Late" broods were
631 enlarged at day 6, and "Control" was the group with not manipulated broods. Black horizontal
632 bars indicate median, whiskers indicate minimum and maximum values, dark grey and light
633 grey colours denote, respectively, females and males.

634

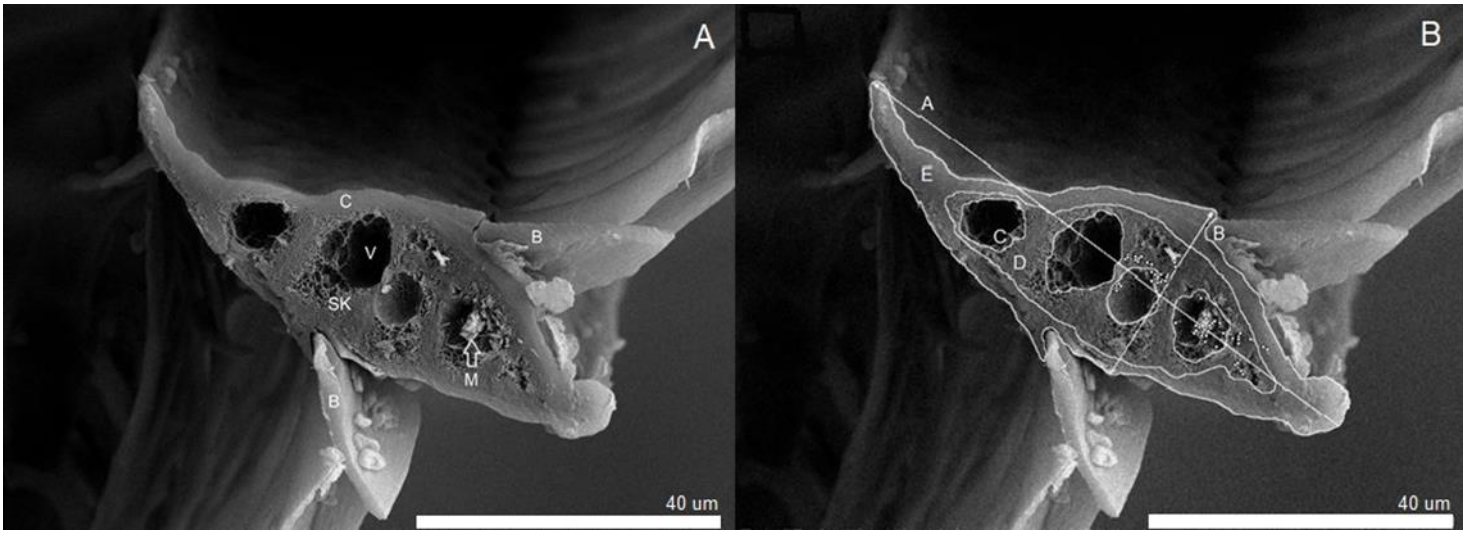

Figure 4. A. SEM images of barb cross-section, with solid keratin cortex (C), spongy keratin nanostructure (SK), air vacuoles (V), melanosomes (M) and barbules (B). **B**. Parameters measured in the ImageJ software: height (A), width (B), area of air cavities (C), medullary area (D), total area (E) and melanosomes (marked with white dots).

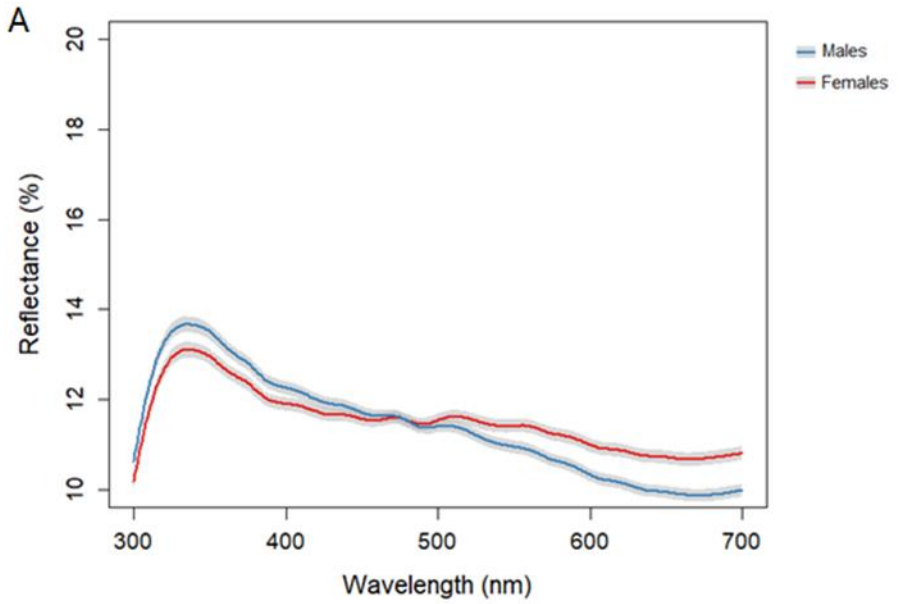
A
Reflectance (%)
10
12
14
16
18
20
300
400
500
600
700
Wavelength (nm)
Males
Females

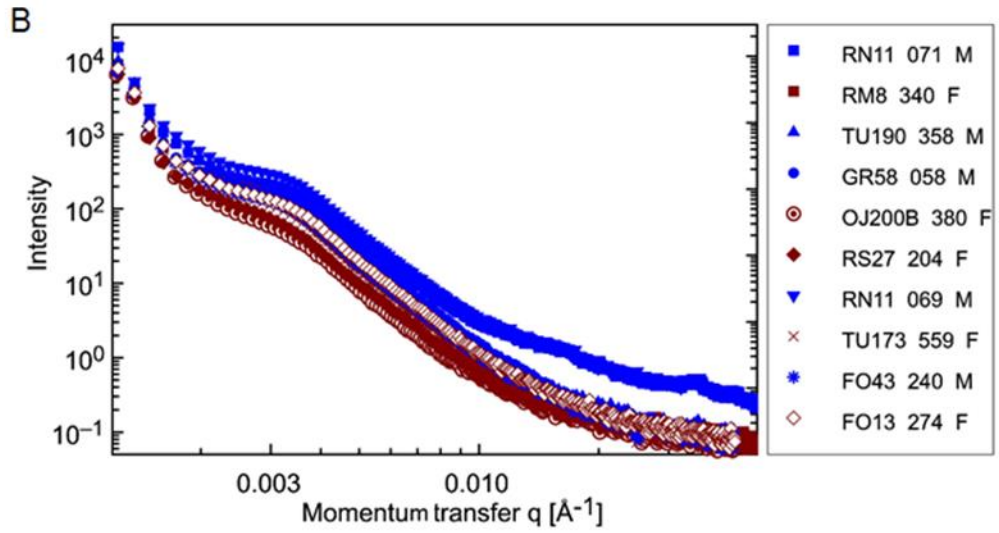
B
Intensity
10^{4}
10^{3}
10^{2}
10^{1}
10^{0}
10^{-1}
0.003
0.010
Momentum transfer q [Å^{-1}]
RN11 071 M
RM8 340 F
TU190 358 M
GR58 058 M
OJ200B 380 F
RS27 204 F
RN11 069 M
TU173 559 F
FO43 240 M
FO13 274 F

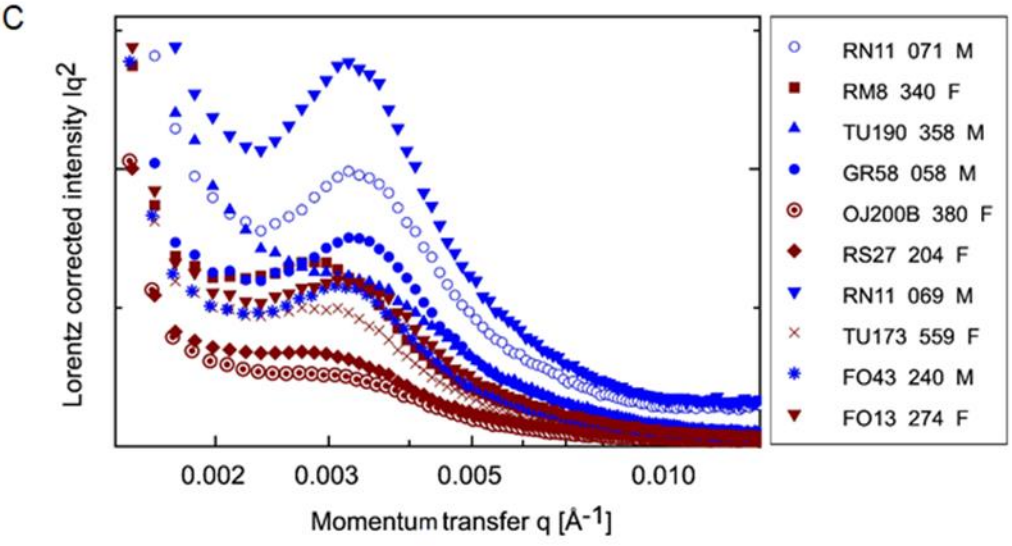
C
Lorentz corrected intensity Iq^2
0.002
0.003
0.005
0.010
Momentum transfer q [Å^{-1}]
RN11 071 M
RM8 340 F
TU190 358 M
GR58 058 M
OJ200B 380 F
RS27 204 F
RN11 069 M
TU173 559 F
FO43 240 M
FO13 274 F

642

Figure 5.A Averaged reflectance spectra of blue tit nestlings tail feather's outer vane. Blue and red lines indicate, respectively male and female mean reflectance, whilst the grey shading indicates standard error. Example SAXS data (**B**) and Lorentz corrected SAXS data (**C**) curves of blue tit nestlings tail feather's outer vane, of ten randomly chosen individuals. Males and females are marked with a blue and red, respectively. Alphanumeric codes represent individual nest-boxes and three last digits their ring numbers.

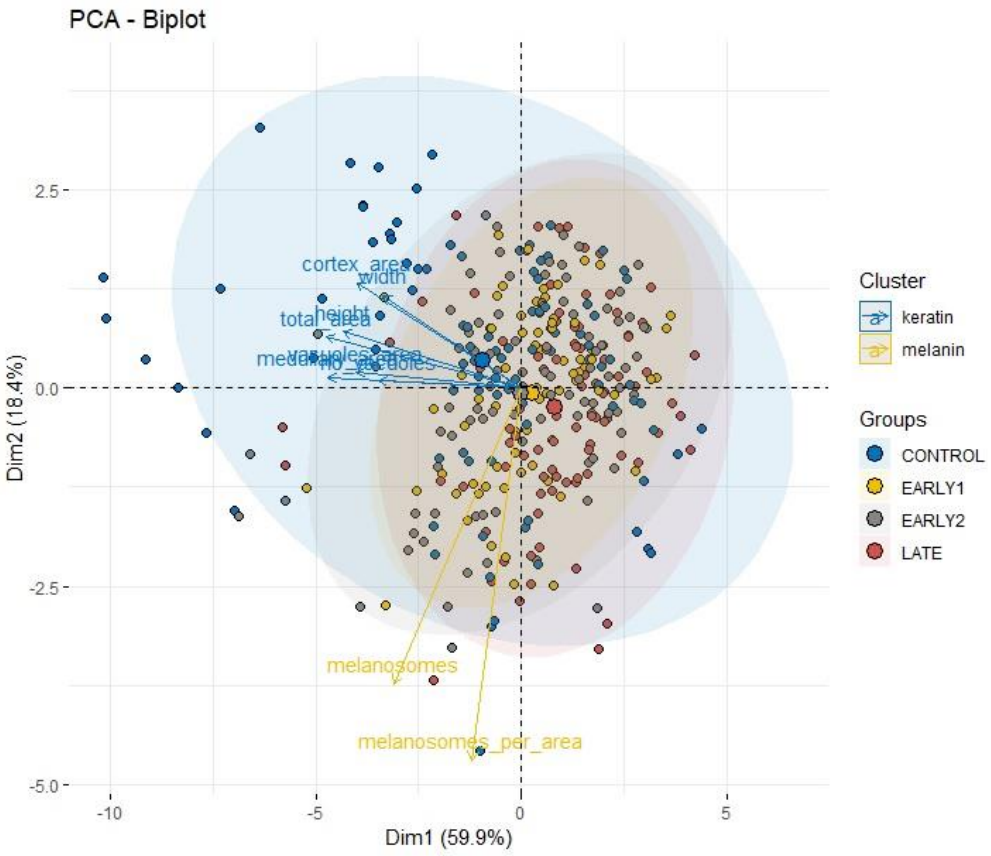

Figure 6. PCA biplot of 352 nestlings tail feathers barb's cross-sections, using all micro-scale characteristics' variables, explained by the two principal component axes, with variables categorized to either keratin or melanin cluster and divided into four experimental groups.